

This is the accepted manuscript made available via CHORUS. The article has been published as:

# Lifetime measurements of low-spin negative-parity levels in $^{160}\text{Gd}$

S. R. Leshner, C. Casarella, A. Aprahamian, L. M. Robledo, B. P. Crider, R. Ikeyama, I. R. Marsh, M. T. McEllistrem, E. E. Peters, F. M. Prados-Estévez, M. K. Smith, Z. R. Tully, J. R. Vanhoy, and S. W. Yates

Phys. Rev. C **95**, 064309 — Published 12 June 2017

DOI: [10.1103/PhysRevC.95.064309](https://doi.org/10.1103/PhysRevC.95.064309)

# Lifetime measurements of low-spin negative-parity levels in $^{160}\text{Gd}$

S.R. Leshner,<sup>1,2,\*</sup> C. Casarella,<sup>2</sup> A. Aprahamian,<sup>2</sup> L. M. Robledo,<sup>3</sup> B. P.

Crider,<sup>4,†</sup> R. Ikeyama,<sup>1</sup> I. R. Marsh,<sup>1</sup> M. T. McEllistrem,<sup>4</sup> E. E. Peters,<sup>5</sup>

F. M. Prados-Estévez,<sup>4,5</sup> M. K. Smith,<sup>2,†</sup> Z. R. Tully,<sup>1</sup> J. R. Vanhoy,<sup>6</sup> and S. W. Yates<sup>4,5</sup>

<sup>1</sup>*Department of Physics, University of Wisconsin – La Crosse, La Crosse, Wisconsin 54601-3742, USA*

<sup>2</sup>*Department of Physics, University of Notre Dame, Notre Dame, Indiana 46556, USA*

<sup>3</sup>*Dep. Física Teórica (Módulo 15), Universidad Autónoma de Madrid, E-28049 Madrid, Spain*

<sup>4</sup>*Department of Physics and Astronomy, University of Kentucky, Lexington, Kentucky 40506-0055, USA*

<sup>5</sup>*Department of Chemistry, University of Kentucky, Lexington, Kentucky 40506-0055, USA*

<sup>6</sup>*Department of Physics, United States Naval Academy, Annapolis, Maryland 21402, USA*

(Dated: May 2, 2017)

$^{160}\text{Gd}(n, n'\gamma)$  experiments were performed with accelerator-produced monoenergetic neutrons. Excitation functions at neutron energies from 1.5 to 2.8 MeV aided in the placement of  $\gamma$  rays in the level scheme and angular distributions at three neutron energies resulted in the determination of twenty eight excited-level lifetimes or limits in  $^{160}\text{Gd}$ , including the lifetimes of several negative-parity levels attributed to octupole vibrations.

## I. INTRODUCTION

The  $^{160}\text{Gd}$  nucleus lies in the well-known rare-earth region of deformation and has an  $R_{4/2} [\equiv E(4_{gs}^+)/E(2_{gs}^+)]$  ratio of 3.30, placing it close to the rotational limit. An open question in nuclear structure is the viability of vibrational excitations in deformed nuclei. The lowest-lying excited vibrational modes include quadrupole and octupole excitations. Single-phonon quadrupole are the  $\gamma$  and  $\beta$  vibrations.  $\gamma$  vibrations seem to be well characterized as the first  $K^\pi = 2^+$  bands and exhibit a systematic behavior across the region of deformed nuclei with typical  $B(E2; 2_\gamma^+ \rightarrow 0_{gs}^+)$  values of a few Weisskopf units (W.u.). In contrast, the  $\beta$  vibrations do not exhibit these systematic characteristics as the  $B(E2)$  values of transitions de-exciting the first excited  $K^\pi = 0^+$  band vary greatly throughout the deformed region [1–3]. The question regarding the viability of the  $\beta$ -vibrations in deformed nuclei remains open to debate [4–9].

Octupole excitations in spherical nuclei are identified by large  $B(E3; 0_{gs}^+ \rightarrow 3^-)$  [10] values, and a compilation of  $B(E3)$  values of the lowest  $3^-$  states can be found in Ref. [11]. In deformed nuclei, the octupole mode splits into  $K^\pi = 0^-, 1^-, 2^-$ , and  $3^-$  bands. The increasing level density with excitation energy and the proximity of the pairing gap complicate the identification of vibrations in deformed nuclei. Two-phonon octupole excitations have been observed in spherical nuclei of the rare-earth region –  $^{144}\text{Sm}$  [12],  $^{146}\text{Sm}$  [13],  $^{146}\text{Gd}$  [14],  $^{147}\text{Gd}$  [15], and  $^{148}\text{Gd}$  [16, 17] – as has the combined two-phonon quadrupole-octupole vibrational mode ( $2^+ \otimes 3^-$ ) in nearly spherical nuclei – *e.g.*,  $^{144}\text{Sm}$  [12],  $^{146}\text{Sm}$  [18], and  $^{148}\text{Gd}$  [13]. A few cases have been suggested as two-phonon double- $\gamma$  vibrations ( $K^\pi = 4^+$ ) in  $^{164}\text{Dy}$  [19],  $^{166}\text{Er}$  [20],  $^{168}\text{Er}$  [21–23], and ( $K^\pi = 0^+$ ) in  $^{166}\text{Er}$  [24]. A two-phonon double- $\beta$  vibration has also been proposed in  $^{178}\text{Hf}$  [25].

The low-lying structure of  $^{160}\text{Gd}$  has been extensively studied; there are numerous positive- and negative-parity bands identified in this nucleus, including an excited  $K^\pi = 2^+$  band, several excited  $K^\pi = 0^+$  bands, and  $K^\pi = 0^-, 1^-,$  and  $2^-$  bands. There is, however, a paucity of level lifetimes and transition probabilities to clearly identify the collectivity or lack thereof for these excitations. Our recent paper reported on the characteristics of the  $K^\pi = 0^+$  states [26] in this nucleus. This work reports mainly on the lifetime measurements of levels in low-lying  $K^\pi = 0^-, 1^-,$  and  $2^-$  bands. Using the Doppler-shift attenuation method following inelastic neutron scattering, we have determined the lifetimes of a large number of excited levels in  $^{160}\text{Gd}$ , many of them for the first time.

---

\*Electronic address: [slesher@uwlax.edu](mailto:slesher@uwlax.edu)

†present address: National Superconducting Cyclotron Laboratory, Michigan State University, East Lansing, Michigan, 48824, USA

## II. EXPERIMENT

The low-lying states of  $^{160}\text{Gd}$  were studied with the  $(n, n'\gamma)$  reaction at the University of Kentucky Accelerator Laboratory (UKAL) with monoenergetic neutrons produced by the  $^3\text{H}(p, n)^3\text{He}$  reaction. The scattering sample was 29.456 g of 98.12% enriched  $^{160}\text{Gd}_2\text{O}_3$  contained in a thin-walled polyethylene cylinder 3.1 cm in height and 2.3 cm in diameter. The emitted  $\gamma$  rays were recorded with a HPGe detector with a relative efficiency of  $\approx 50\%$ . A bismuth germanate (BGO) active shield was used for Compton suppression. The HPGe detector was located at a distance of 119.3 cm from the scattering sample, and time-of-flight gating was used to suppress background radiation. Standard radioactive sources,  $^{226}\text{Ra}$  and  $^{152}\text{Eu}$ , were used for energy and efficiency calibration. In angular distribution measurements, a  $^{60}\text{Co}$  source was placed near the detector as a continuous check on gain stability. At higher neutron energies,  $^{24}\text{Na}$  was used as an additional in-beam source for accurate energy determination. Additional descriptions of the experimental setup and techniques are documented in Refs. [27–29].

The excitation function measurement provided yields of  $\gamma$  rays as a function of incident neutron energy ( $E_n$ ), and spectra were measured for  $E_n = 1.5$  to 2.8 MeV in 80- or 100-keV steps, with the detector at  $90^\circ$  with respect to the beam axis. Examples of the excitation functions obtained for  $\gamma$  rays from the same level are shown in Fig. 1. Excitation thresholds were used to place  $\gamma$  rays and establish levels. Angular-distribution spectra were recorded at neutron energies of 1.5, 2.0, and 2.8 MeV at ten angles over a range of  $40^\circ$  to  $150^\circ$ . To obtain the most accurate lifetimes, these neutron energies were chosen to minimize feeding to the levels of interest. The angular distributions of the  $\gamma$ -ray intensities,  $W(\theta)$  were fitted with a function of even-order Legendre polynomials,

$$W(\theta) = A_o [1 + a_2 P_2(\cos \theta_\gamma) + a_4 P_4(\cos \theta_\gamma)], \quad (1)$$

where the parameters  $a_2$  and  $a_4$  depend on the multipolarities and mixing amplitudes of the transitions. The experimental values of these parameters were then compared to statistical model calculations from the code CINDY [30] to determine multipole mixing ratios ( $\delta$ ) of the transitions. If the intensity of the  $\gamma$  ray was small or if the statistical uncertainty was large, the  $a_2$  and  $a_4$  values were compared with those in Govor, *et al.* [31]. Provided the values matched within uncertainties, the values of Ref. [31] were used in relevant calculations and noted.

The angular distribution measurements were also used to extract lifetimes of excited states shorter than about 1 ps by the Doppler-shift attenuation method (DSAM) [32]. The energies of the  $\gamma$  rays have an angular dependence described by

$$E_\gamma(\theta_\gamma) = E_{\gamma 0} \left[ 1 + \frac{v_{cm}}{c} F(\tau) \cos \theta_\gamma \right] \quad (2)$$

where  $E_{\gamma 0}$  is the unshifted  $\gamma$ -ray energy,  $v_{cm}$  is the recoil velocity of the center-of-mass,  $\theta_\gamma$  is the angle of observation, and  $F(\tau)$  is the attenuation factor, which depends on the stopping powers. By examining the energy of a  $\gamma$  ray as a function of angle, the  $F(\tau)$  value can be extracted and compared with those calculated using the Winterbon stopping power formalism [33], and the lifetime of the state,  $\tau$ , can be obtained. An extensive discussion on the DSAM can be found in Ref. [32].

## III. RESULTS

The levels, depopulating transitions, multipole mixing ratios, lifetimes, and resulting  $B(E\lambda)$  transition probabilities are listed in Table I. Energies given for the  $\gamma$  rays were obtained from the angular distribution measurements at the lowest incident neutron energy for which the  $\gamma$ -ray yields were observed to have good statistics. This procedure allowed for accurate energies of peaks which may evolve into complex structures at higher incident neutron energies. The branching ratios and lifetimes were also obtained at the lowest feasible neutron energies. The level energies were determined by a weighted least-squares fit of all the  $\gamma$  rays to and from a level.

Since the last evaluation of  $^{160}\text{Gd}$  [34], three papers have made additions to the  $^{160}\text{Gd}$  level structure using the  $(n, n'\gamma)$  reaction [26, 31, 35]. This information has been considered along with the current results and is presented in Table I. Gamma rays from a level were only included if the excitation functions were consistent in shape and threshold for all  $\gamma$  rays. There were also previously placed  $\gamma$  rays that were below our experimental observation threshold and these were not included in the level scheme [31].

In the following sections, we discuss levels which are germane to the  $K^\pi = 2_\gamma^+$  band and the negative-parity bands in  $^{160}\text{Gd}$ . A partial level scheme is shown in Fig. 2.

### A. $K^\pi = 2_\gamma^+$ band

The  $2_\gamma^+$  bandhead at 988.72 keV had a previously measured level lifetime of 1876(87) fs. This value is the weighted average of four Coulomb excitation experiments [36–39] as given in the latest nuclear data compilation of A=160 [34]. We observed three  $\gamma$  rays from this level, but only the 913.43- and 988.68-keV  $\gamma$  rays were used in extracting the level lifetime limit of  $> 1800$  fs. This value is near the limit of our method, but is consistent with the accepted literature value. The 739.96-keV  $\gamma$  ray is near the energy of a background  $\gamma$  ray and, therefore, was not used in determining the level lifetime. In Table I, transition probabilities were calculated using the literature lifetime and the associated branching ratios from Ref. [31] to calculate the  $B(E2)$  values presented, after ensuring the consistency of the reported branching ratios with our data.

The  $4_\gamma^+$  member of the band at 1148.15 keV depopulates by 899.59- and 1072.85-keV  $\gamma$  rays. Govor *et al.* [31] observed a doublet at a  $\gamma$ -ray energy of 632.89 keV, which they placed as decays from both the 1148.14- and 1621.44-keV levels. From the excitation function shape and threshold, our work assigns this  $\gamma$  ray to the 1621.56-keV level.

The level at 1148.15 keV is assigned as  $J^\pi = 4^+$  from polarized proton scattering measurements, and the authors concluded a hexadecapole component for this state [40]. Our work yields a level lifetime  $\tau = 1080_{-320}^{+730}$  fs, leading to  $B(E2; 4_\gamma^+ \rightarrow 4_{gs}^+) = 16_{-10}^{+5}$  W.u. and  $B(E2; 4_\gamma^+ \rightarrow 2_{gs}^+) = 3.8_{-1.1}^{+2.6}$  W.u., consistent with the expected quadrupole collectivity of this level and the  $K^\pi = 2^+$   $\gamma$  bands in the rare-earth deformed region of nuclei.

The 1261.24-keV  $5_\gamma^+$  level decays to the ground-state band,  $B(E2; 5_\gamma^+ \rightarrow 4_{gs}^+) = 35_{-12}^{+8}$  W.u. and  $B(E2; 5_\gamma^+ \rightarrow 6_{gs}^+) = 31_{-10}^{+7}$  W.u. The ratios of these transition probabilities are consistent, within error, with the Alaga rules.

### B. $K^\pi = 0^-$ band

The  $3_1^-$  level at 1289.90 keV de-excites by two  $\gamma$  rays, 1041.37 and 1214.79 keV. The 1214.79-keV  $\gamma$  ray is observed with an  $a_2 = -0.276(33)$ , which supports the assignment of an  $E1$  transition. Ref. [31] assigns the 1214.79-keV  $\gamma$  ray as a doublet, but we see only a single  $\gamma$  ray in our measurements. A lifetime of  $\tau = 74 \pm 20$  fs was reported from Coulomb excitation and Doppler-broadening measurements [39], but our value of  $\tau = 34 \pm 3$  fs is not in agreement with this value. An advantage of the  $(n, n'\gamma)$  reaction with accelerator-produced neutrons of variable energies is the ability to nonselectively populate levels up to the incident neutron energy. By determining the lifetime of the 1289.90-keV level at  $E_n = 1.5$  MeV, the feeding of the level has been greatly reduced from levels with significantly longer lifetimes. If the neutron energy is increased to 2.0 MeV, increasing feeding from higher levels, the apparent lifetime is increased to  $\tau = 60 \pm 10$  fs. The method of selecting the neutron energy for population of the level gives us confidence in our measured lifetime values. The  $K^\pi = 0^-$  band with  $1_1^-$ ,  $3_1^-$ ,  $5_1^-$  members at 1224.33, 1289.90, and 1427.40 keV, respectively, decay by  $E1$  transitions to the ground-state band.  $E1$  transitions to the  $\gamma$  band were not observed.

### C. $K^\pi = 1^-$ band

The 1351.30-keV level is the bandhead of the  $K^\pi = 1^-$  band and was introduced in Ref. [41] by the placement of 1351.0- and 1275.90-keV  $\gamma$  rays. We observe both of these  $\gamma$  rays, and our spectra are not complicated by the doublet at 1351.09 keV reported in Ref. [31]. We determine a level lifetime of  $\tau = 180 \pm 20$  fs.

A level at 1388.64 keV was assigned by Berzin *et al.* [41] with five de-exciting  $\gamma$  rays, where those at 1388.7 and 1313.0 keV were the most intense. In later work [31], this level was rejected on the basis of a measured angular distribution and the 1388.56-keV  $\gamma$  ray was assigned to a new  $3^-$  level at 1464.00 keV. This 1464.00-keV level was assigned as a  $J^\pi = 3^-$  member of the  $1^-$  band [31]. The 1388.75-keV  $\gamma$  ray has an excitation threshold of 1.5 MeV which favors the placement from the 1464.00-keV level with an  $a_2$  value in agreement with Ref. [31]. Further evidence to support the removal of the 1388.7-keV level is obtained from the  $\gamma$  ray at 1313.03 keV. The excitation threshold is higher than for the 1388.64-keV  $\gamma$  ray and is consistent with the placement at the 1561.63-keV level. Our data do not support any other decays to or from the 1388.7- or the 1464.00-keV level. The 1388.64-keV level has been removed from the level scheme.

### D. $K^\pi = 2^-$ band

A  $K^\pi = 2^-$  band was proposed in Ref. [35] with levels at 1621.4 keV ( $2^-$ ), 1691.4 keV ( $3^-$ ), 1782.5 keV ( $4^-$ ), and 1884.2 keV ( $5^-$ ).

In Ref. [31], a doublet at 632.82 keV was reported and the  $\gamma$  rays were placed from the 1148.14-keV level ( $4^+_\gamma$ ) and a 1621-keV level. The energy thresholds in our data support placement at 1621.56 keV. Unlike Ref. [31], the 632.94-keV  $\gamma$  ray is a singlet with  $a_2 = 0.180(42)$  and  $a_4 = -0.030(69)$ . CINDY calculations support the placement of both the 632.94- and 564.06-keV  $\gamma$  rays to a  $J^\pi = 2^-$  state in agreement with Ref. [35].

The  $\gamma$  rays observed in this work from the  $3^-$  level at 1691.68 keV agree with those proposed in Ref. [31]. We observe a level lifetime of  $\tau = 230^{+350}_{-100}$  fs with a preferred decay to the  $\gamma$  band,  $B(E1; 3^-_4 \rightarrow 4^+_\gamma) = 2^{+1}_{-3}$  mW.u.,  $B(E1; 3^-_4 \rightarrow 3^+_\gamma) = 2.1^{+0.9}_{-3.2}$  mW.u., and  $B(E1; 3^-_4 \rightarrow 2^+_\gamma) = 1.5^{+0.7}_{-2.3}$  mW.u.

The  $4^-$  level at 1782.67 keV was proposed in Ref. [35]. We confirm the placement of the 725.19 and 521.53 keV  $\gamma$  rays but are unable to calculate a lifetime due to low statistics.

Recent studies of quadrupole and octupole states in  $^{168}\text{Yb}$  ( $R_{4/2} = 3.27$ ) noted a pattern of strong decay from a  $K^\pi = 2^-$  band into the  $\gamma$ -vibrational band when compared to the decay into the ground-state band [42]. This is consistent with the degree of K forbiddenness. Earlier work by Aprahamian [43] showed a difference of three orders of magnitude in  $E1$  strength for transitions between states with the same K ( $\Delta K = 0$ ) and for those with  $\Delta K = 2$ . The authors note [42] this interesting decay pattern has also been observed in the  $J^\pi = 2^-$  states belonging to the  $K^\pi = 2^-$  band in the nuclei from Gd ( $Z = 64$ ) to W ( $Z = 74$ ). The preferred decay  $^{168}\text{Yb}$  is to the  $J^\pi = 4^-$  state. Providing more evidence of a  $K^\pi = 2^-$  band. The enhanced  $E1$  transitions indicate some overlap with the  $\gamma$  band but further study of the negative-parity states, including  $E3$  strengths, are needed.

### E. $K^\pi = 0^+$ bands

The  $0^+$  states in  $^{160}\text{Gd}$  were discussed in Ref. [26].  $0^+$  states at 1379.7 and 1558.3 keV were confirmed and assigned lifetime limits of  $> 1350$  and  $> 590$  fs, respectively, and states at 1325.73 and 2236 keV were rejected as possible  $0^+$  states. The band structure of these levels was also explored and is included in Table I.

After evaluation of the full angular distribution data set at neutron energies of 1.5, 2.2, and 2.8 MeV, the  $F(\tau)$  values were scrutinized. From a careful evaluation of the full data set, only  $F(\tau)$  values with uncertainties which overlapped the other values were used in the lifetime calculation. This process led to the recalculation of the lifetime of the 1599.05-keV level. The re-evaluated value of  $\tau = 800^{+730}_{-300}$  fs is consistent with our formerly published limit of  $> 300$  fs [26], albeit with a large uncertainty. The  $\gamma$  rays of 1599.05 keV and 988.72 keV overlap with background lines and were not observed in this set of experiments.

### F. Discussion

We have studied levels in  $^{160}\text{Gd}$  with the  $(n, n'\gamma)$  reaction. Excitation functions aided in the placement of  $\gamma$  rays in the level scheme and angular distributions resulted in the determination of multipole mixing ratios and level lifetimes of excited states and, hence, the depopulating  $B(E2)$  and  $B(E1)$  values for transitions from  $K^\pi = 0^+, 2^+, 4^+, 0^-, 1^-$ , and  $2^-$  bands. In a previous paper [26], we identified excited  $K^\pi = 0^+$  band heads at 1379 and 1558 keV and the excited levels built on them. The measured lifetimes for the first and second excited  $K^\pi = 0^+$  band members were determined as limits. Nonetheless, the limits indicate potentially enhanced collective transitions from the  $2^+$  and  $4^+$  members of the band. In this work, we have measured the level lifetimes for several members of the negative-parity bands. Figure 3 shows the revised lifetime of the  $2^+$  state of the  $K^\pi = 0^+$  band at 1599 keV with an enhanced  $B(E2)$  of  $41^{+16}_{-37}$  W.u. connecting this state to the  $K^\pi = 2^+$  band member, the  $3^+$  state at 1057. This kind of enhanced  $B(E2)$  transition probability could be due to a collective excitation built on the  $K^\pi = 2^+$  band.  $B(E2)$  values to the ground state band are 100 times weaker.

The lifetimes of the excited states in negative-parity bands are listed in Table I. A partial level scheme is shown for the depopulation of the negative-parity bands for  $K^\pi = 0^-, 1^-$ , and  $2^-$  bands along with the  $K^\pi = 2^+$   $\gamma$  band. These transitions are  $E1$  in nature and show  $B(E1)$  values that are strongly enhanced for the  $K=0^-$  band depopulating on the order of a few mW.u. These are three orders of magnitude more enhanced than typical  $E1$  values in deformed nuclei [43, 44]. In comparison, the negative-parity bands with  $K^\pi = 1^-$  and  $2^-$  are one and two orders of magnitude weaker in  $B(E1)$ 's to the ground-state band while the  $K^\pi = 2^-$  band member at 1692 shows enhanced  $E1$  transitions connecting this level to the  $K^\pi = 2^+$  band. The Alaga values for the ratio of  $B(E1; 1^-_{K^\pi=0^-} \rightarrow 2^+_{gs})$  to  $B(E1; 1^-_{K^\pi=0^-} \rightarrow 0^+_{gs})$  is 2.0 and the experimental ratio is 1.7.

A disagreement over the assignment of the 1622-keV between Ref. [31] ( $J^\pi = 4^+$ ) and Ref. [35] ( $J^\pi = 2^-$ ) can be addressed. The current data supports the  $2^-$  assignment and experimental  $B(E1; 2^-_{K^\pi=2^-} \rightarrow 3^+_{K^\pi=2^+})$  to  $B(E1; 2^-_{K^\pi=2^-} \rightarrow 2^+_{K^\pi=2^+})$  of 0.41 in good agreement with the theoretical Alaga value of 0.36. Similarly, the  $B(E1; 3^-_{K^\pi=0^-} \rightarrow 4^+_{gs})$  to  $B(E1; 3^-_{K^\pi=0^-} \rightarrow 2^+_{gs}) = 1.3$  and the experimental  $B(E1)$  ratio is 0.9 in good agreement

within errors. The ratio of  $B(E1; 3_{K^\pi=2^-}^- \rightarrow 4_{K^\pi=2^+}^+)$  to  $B(E1; 3_{K^\pi=2^-}^- \rightarrow 3_{K^\pi=2^+}^+)$  to  $B(E1; 3_{K^\pi=2^-}^- \rightarrow 2_{K^\pi=2^+}^+)$  for the 1691.68 keV level to the  $4^+, 3^+, 2^+$  members of the  $K^\pi = 2^+ \gamma$  band, should be 1.8:1.4:1.0 from the Alaga rules and the experimental equivalent is 1.3:1.4:1.

The agreement of the Alaga rules with the measured  $B(E1)$  values at 1692 as the  $3^-$  member of a  $K^\pi = 2^-$  band is further evidence of the  $K^\pi = 2^-$  assignment. If the 1691.68-keV level belongs to a  $K^\pi = 3^-$  band, then the Alaga ratio would be 0.05:0.35:1, in complete disagreement with measured values.

The collective quadrupole and octupole degrees of freedom were analyzed in  $^{160}\text{Gd}$  using the well-known Generator Coordinate Method (GCM) with the Gogny D1S energy density function. Mean-field Hartree-Fock-Bogoliubov (HFB) constrained calculations were carried out using the axially symmetric quadrupole and octupole mass moments in order to explore the shape of the potential energy surface (PES) and to check for the existence of octupole deformed minima. An in-depth discussion of this method can be found in Ref. [44–46]. The computed PES reveals a reflection symmetric (i.e., with zero octupole deformation) for the ground state but the PES along the octupole direction is rather soft indicating the need of a beyond-mean-field calculation using the GCM. Fig. 4 shows a deep minimum potential well that is quadrupole deformed. The lowest oblate minimum does not appear until 5 MeV. The calculations show a first excited  $K=0^-$  state appears at an excitation energy of 1.84 MeV with a  $B(E1; 1_{K^\pi=0^-}^- \rightarrow 0_{gs}^+)$  value of 5.1 mW.u., as shown in Fig. 5a. The  $B(E3; 3^- \rightarrow 0_{gs}^+) = 13.50$  W.u. The second excited  $0^+$  state is a one-phonon  $\beta$  vibration with an excitation energy of 3.36 MeV and the  $2^+$  member decays to the ground state with a  $B(E2; 2^+ \rightarrow 0_{gs}^+) = 3.7$  W.u. and the  $10^3 \rho^2$  ( $E_0$ ) transition strength of 230. The third excited  $0^+$  state in this calculation is a two-octupole phonon at 3.94 MeV with a  $B(E2; 2^+ \rightarrow 0_{gs}^+) = 0.71$  W.u. and an  $10^3 \rho^2$  ( $E_0$ ) = 9. These calculated values are compared with the experimental values in Fig. 5. We have not measured any E3 transitions in this work, but the  $B(E3)$  value used in comparison was established previously. Our experimental level scheme is compressed in comparison to the GCM calculations. There is, however, very good agreement between the calculated and experimental  $B(E1; 1_{K^\pi=0^-}^- \rightarrow 0_{gs}^+)$  values. The prediction is for an excited  $K^\pi = 0^+$  band at 3.9 MeV as a double octupole phonon built on the  $K^\pi = 0^-$  band at 1840 keV. Our work shows an excited  $K^\pi = 0^+$  band at 1558 keV that is connected to the first excited  $K^\pi = 2^+$  band as shown in Table I and Fig. 3. All indications are that this  $K^\pi = 0^+$  band at 1558 keV is the double-phonon  $\gamma\gamma$  vibrational band. The  $K^\pi = 2^+ \gamma$  band head is at 989 keV. The two-phonon  $\gamma\gamma$  vibration in this case is 1.6 times the energy of the single  $\gamma$ -vibrational band. Negative anharmonicities similar to this have been observed in  $^{232}\text{Th}$  [47] in the actinide region and  $^{178}\text{Hf}$  [25] in the rare earths.

#### IV. SUMMARY

We report the results of  $(n, n'\gamma)$  measurements in the low-lying excitation energy regime of  $^{160}\text{Gd}$ . Transition probabilities were calculated from the level lifetimes and, where possible, multipole mixing ratios are determined. The  $B(E2)$  values from the  $K^\pi = 2^+ \gamma$  band indicate that this is indeed a quadrupole collective vibrational excitation. The level lifetimes of the  $4^+$  and  $5^+$  members of this band show transition rates consistent with other  $K^\pi = 2^+ \gamma$ -vibrational bands in this region of deformed nuclei. Our characterization of the 1599.05-keV level with a revised multipole mixing ratio and the assignment or placement of the transitions to the  $\gamma$  band, would make the  $B(E2; 2_4^+ \rightarrow 3_7^+) = 41_{-37}^{+16}$  W.u., potentially pointing to a two-phonon  $\gamma\gamma$ -vibrational character for the  $K^\pi = 0^+$  band at 1558.31 keV. The uncertainty on this  $B(E2)$  value is large, but the observed collective strength, indicating a preferred decay to the  $K^\pi = 2^+ \gamma$  band is difficult to ignore.

In deformed nuclei, low-lying negative-parity states are generally associated with octupole vibrations, and a simple pattern of  $K^\pi = 0^-, 1^-, 2^-$ , and  $3^-$  bands is frequently seen. In pioneering work, Neergård and Vogel [48] described the octupole states in deformed nuclei microscopically, and Barfield, Wood, and Barrett [49] treated the detailed spectra and  $E3$  transition rates of nuclei in the rare earth region within the interacting boson model. Modern approaches to the problem, like the ones used in this paper are required for a more robust prediction of transition strengths and excitation energies of the negative parity states.

Experimentally, octupole bands are identified by enhanced  $E3$  transitions between the  $J^\pi = 3^-$  member of the band and the ground state in spherical nuclei. The compilation of experimental data by Spear [50] and the update by Kibédi and Spear [11] give the excitation energies of the  $3^-$  states and reduced electric octupole transition probabilities,  $B(E3; 0_1^+ \rightarrow 3_1^-)$ , for the first  $3^-$  states of even-even nuclides. Moreover, it is frequently found that known octupole states are populated strongly in single-nucleon transfer reactions, indicating that these states have a complex character with one or more large two-quasiparticle components. While a number of  $E1$  transition rates from negative-parity states are reported in this work, the correlation between these  $B(E1)$ s and octupole strength is less straightforward than that for the  $B(E3)$ s. We note that for example, the 1224.33- and 1289.90-keV levels of the  $K^\pi = 0^-$  band have de-exciting transitions of several mW.u. compared to the  $1^-$  band where the  $B(E1)$ s are less than 1 mW.u. Structural assignments based solely on  $B(E1)$  values should be made with caution [51]; therefore, we note these values, along

with the previous reported  $B(E3; 3^- \rightarrow 0_{gs}^+) = 11.1(7)$  W.u. [39], indicate an octupole vibration. However, no new  $B(E3)$  values are available from the current work. Also of note is a preferred  $\Delta K = 0$  decay from the  $K^\pi = 2^-$  band to the  $K^\pi = 2^+$   $\gamma$  band from the  $3^-$  state at 1691.68 keV.

Although the energies of the calculated bands in the GCM are higher than the experimental results, the agreement in the transition probabilities suggesting the population of a one-phonon  $\beta$  vibration and a two-octupole phonon state is striking. Further work is underway to include two-quasiparticle excitations in the GCM. New measurements of extended  $B(E2)$  and  $B(E0)$  values in  $^{160}\text{Gd}$  can further clarify the situation.

### A. Acknowledgements

We thank H. E. Baber for his contributions to accelerator maintenance and operation. This material is based upon work supported by the National Science Foundation under Grant Nos. PHY-1606890, PHY-1419765, PHY-1205412, PHY-1507053, PHY-1068192, and PHY-1305801. L. M. Robledo has been supported in part by Spanish grants No. FPA2015-65929-P/MINECO and FIS2015-63770-P/MINECO. The enriched isotope used in this research was supplied by the United States Department of Energy Office of Science by the Isotope Program in the Office of Nuclear Physics.

TABLE I: Energy levels ( $E_L$ ) observed in the  $^{160}\text{Gd}(n,n'\gamma)$  measurements.  $I_\gamma$  is the relative  $\gamma$ -ray intensity;  $F(\tau)$  is the experimental attenuation factor; lifetimes,  $\tau$ , are mean lives in fs. Multipole mixing ratios,  $\delta$ , are obtained in fits to measured angular distributions. When two values are given, they have similar  $\chi^2$  values. If one value is in brackets, the one with the smaller  $\chi^2$  value is given first and is the  $\delta$  value adopted. Literature lifetime values ( $\tau_{lit}$ ) are taken from [34] unless otherwise noted and are shown under the measured lifetime. Parentheses denote tentative assignments or placements. For reference,  $B(E1)_{mW.u.} = 0.190 e^2b$  and  $B(E2)_{W.u.} = 5.16 \times 10^{-7} e^2b^2$ .

$E_L$ (keV)	$J_i^\pi, K$	$J_f^\pi, K$	$E_\gamma$ (keV)	$I_\gamma$	$F(\tau)$	$\tau$ (fs)	Mult.	$\delta$	$B(E1)$ ( $\times 10^{-3}$ W.u.)	$B(E2)$ (W.u.)	Notes
75.24(5)	$2_{gs}^+, 0$	$0_{gs}^+, 0$	75.26	100		$\tau_{lit} = 3.9 \times 10^6$					
248.55(6)	$4_{gs}^+, 0$	$2_{gs}^+, 0$	173.34(5)	100							
515.00(8)	$6_{gs}^+, 0$	$4_{gs}^+, 0$	266.52(5)	100							
988.72(6)	$2_\gamma^+, 2$	$4_{gs}^+, 0$	739.96(7)	< 2	0.008(14)	> 1800	$E2$			0.96(7)	1, 2 3
						$\tau_{lit} = 1876(87)$					
		$2_{gs}^+, 0$	913.43(5)	100(1)			$E2/M1$	$-0.45^{+0.04}_{-0.05}$		$1.2^{+0.22}_{-0.18}$	
		$0_{gs}^+, 0$	988.68(5)	88.7(10)			$E2$	—		4.1(2)	2
1057.42(6)	$3_\gamma^+, 2$	$4_{gs}^+, 0$	809.06(5)	20.6(2)	0.011(13)	> 2200	$E2/M1$	0.11(3)		< 0.04	2
		$2_{gs}^+, 0$	982.28(5)	100(1)			$E2/M1$	$47^{+18}_{-10}$		< 6.5	4
1070.57(7)	$4_1^+, 4$	$6_{gs}^+, 0$	555.45(8)	1.6(1)							
		$4_{gs}^+, 0$	822.06(5)	100(2)							
		$2_{gs}^+, 0$	995.30(5)	64.2(13)							
1148.15(7)	$4_\gamma^+, 2$	$4_{gs}^+, 0$	899.59(5)	100(1)	0.037(15)	$1080^{+730}_{-320}$	$E2/M1$	$21^{+21}_{-7}$		$16^{+5}_{-10}$	4
		$2_{gs}^+, 0$	1072.85(5)	58.5(9)			$E2$	—		$3.8^{+2.6}_{-1.1}$	
1224.33(6)	$1_1^-, 0$	$2_{gs}^+, 0$	1149.12(5)	100(1)	0.676(7)	$20 \pm 2$	$E1$	—	6.5(6)		
						$\tau_{lit} = 21.6(60)$					
		$0_{gs}^+, 0$	1224.38(5)	67.5(8)			$E1$	—	3.6(4)		
1261.24(9)	$5_\gamma^+, 2$	$6_{gs}^+, 0$	746.34(6)	19.6(9)	0.101(26)	$350^{+120}_{-80}$	$E2/M1$	$8^{+13}_{-4}$		$31^{+7}_{-11}$	
								$[0.24(10)]$		$1.7^{+1.4}_{-1.5}$	
		$4_{gs}^+, 0$	1012.65(5)	100(1)			$E2/M1$	$15^{+17}_{-6}$		$35^{+8}_{-12}$	5
1289.90(7)	$3_1^-, 0$	$4_{gs}^+, 0$	1041.37(5)	54.6(7)	0.565(19)	$34 \pm 3$	$E1$	—	3.0(3)		
						$\tau_{lit} = 74(20)$					
		$2_{gs}^+, 0$	1214.79(5)	100(1)			$E1$	—	3.5(3)		
1351.30(6)	$1_2^-, 1$	$2_{gs}^+, 0$	1276.06(5)	100(2)	0.184(8)	$180 \pm 20$	$E1$	—	0.74(8)		
		$0_{gs}^+, 0$	1351.30(5)	20.0(4)			$E1$	—	0.12(1)		
1376.70(8)	$2_1^-, 1$	$3_\gamma^+, 2$	319.38(6)	1.8(1)	0.035(47)	> 550	$E1$	—	< 0.18		2, 6
		$2_{gs}^+, 0$	1301.46(5)	100(1)			$E1$	—	< 0.27		
1379.71(10)	$0_2^+, 0$	$2_{gs}^+, 0$	1304.46(5)	100	0.015(14)	> 1350	$E2$	—		< 3.1	7
1427.40(12)	$5_1^-, 0$	$4_{gs}^+, 0$	1178.85(6)	100	0.514(69)	$50 \pm 10$	$E1$	—	4.0(8)		
1436.34(7)	$2_2^+, 0$	$4_{gs}^+, 0$	1187.81(5)	100(1)	0.036(28)	> 340	$E2$	—		< 13	7
		$2_{gs}^+, 0$	1361.05(6)	36.4(4)			$E2/M1$	0.00(8)		< 2.4	
								$[2.4^{+0.6}_{-0.4}]$		< 2.0	
		$0_{gs}^+, 0$	1436.34(6)	13.5(2)			$E2$	—		< 0.70	6
1464.00(10)	$3_2^-, 1$	$2_{gs}^+, 0$	1388.75(5)	100	0.344(43)	$50 \pm 5$	$E1$	—	2.5(2)		

continued

TABLE I: *continued*

$E_L$ (keV)	$I_i^\pi, K$	$I_f^\pi, K$	$E_\gamma$ (keV)	$L_\gamma$	$F(\tau)$	$\tau$ (fs)	Mult.	$\delta$	$B(E1)$ ( $\times 10^{-3}$ W.u.)	$B(E2)$ (W.u.)	Notes
1498.94(10)	$4_1^-, 1$	$4_{gs}^+, 0$	1250.39(5)	100	0.053(51)	$> 400$	$E1$	—	$< 0.41$		6
1532.29(13)	$3_3^-, (3)$	$4_1^+, 2$	384.14(6)	100	—	—					6
		$4_{gs}^+, 0$	1283.10(8)	—							9
1558.31(12)	$0_3^+, 0$	$2_{gs}^+, 0$	1483.06(6)	100	0.004(69)	$> 590$	$E2$	—		$< 3.7$	7
1561.63(10)	$4_3^+, 0$	$6_{gs}^+, 0$	1046.67(6)	100(1)	0.049(53)	$> 320$	$E2$	—		$< 22$	7
		$4_{gs}^+, 0$	1313.03(6)	74.8(3)			$E2/M1$	$0.28^{+0.34}_{-0.12}$		$< 0.40$	
1568.77(6)	$1_1^+, 1$	$1_2^-, 1$	217.51(6)	8.8(15)	0.044(28)	$1000^{+1800}_{-400}$	$E1$	—	$0.97^{+0.7}_{-1.8}$		2, 6
		$2_\gamma^+, 2$	580.20(6)	89.2(16)			$E2/M1$	$0.28^{+0.25}_{-0.18}$		$5.3^{+6.7}_{-13}$	
		$2_{gs}^+, 0$	1493.40(6)	94.4(16)			$E2/M1$	$1.34^{+1.6}_{-0.6}$		$0.44^{+0.23}_{-0.88}$	
		$0_{gs}^+, 0$	1568.70(6)	100(2)			$M1$	—			
1586.61(12)	$2_3^+, 1$	$2_{gs}^+, 0$	1511.36(6)	100	0.044(39)	$> 500$	$E2/M1$	—		$< 4.01$	6
1599.05(6)	$2_4^+, 0$	$3_1^-, 0$	309.32(6)	8.9(4)	0.056(26)	$800^{+730}_{-300}$	$E1$	—	$0.34^{+0.13}_{-0.31}$		8, 6
		$1_1^-, 0$	374.78(6)	14.8(3)			$E1$	—	$0.32^{+0.12}_{-0.29}$		
		$3_\gamma^+, 2$	541.53(6)	36.8(3)			$E2/M1$	$-5.57^{+1.91}_{-5.00}$		$41^{+16}_{-37}$	
								$-0.01(9)$		$0.004(77)$	
		$2_{gs}^+, 0$	1523.59(6)	100(1)			$E2/M1$	$-1.04^{+0.22}_{-2.10}$		$0.34^{+0.68}_{-0.32}$	
		$0_{gs}^+, 0$	1598.85(6)	78.7(1)			$E2$	—		$0.41^{+0.15}_{-0.37}$	
1621.56(9)	$2_2^-, 2$	$3_1^+, 2$	564.06(6)	29.0(7)	0.167(155)	$240^{+3600}_{-140}$	$E1$	—	$1.7^{+0.6}_{-0.1}$		10
		$2_\gamma^+, 2$	632.94(6)	100(2)			$E1$	—	$4.2^{+1.4}_{-0.3}$		
1648.06(12)	$4_5^+$	$2_{gs}^+, 0$	1572.81(6)	100	0.134(58)	$300^{+260}_{-100}$	$E2$	—		$5.5^{+2.8}_{-2.6}$	6
1653.32(12)	$5_2^-, 1$	$6_{gs}^+, 0$	(1138.51(6))	—	0.454(78)	$60^{+20}_{-15}$					2, 6
		$4_{gs}^+, 0$	1404.77(6)	100							
1661.75(9)		$4_{gs}^+, 0$	1413.16(7)	5.6(2)	0.050(32)	$880^{+1600}_{-360}$					9, 6
		$2_{gs}^+, 0$	1586.52(6)	100(1)							
1691.68(7)	$3_4^-, 2$	$4_\gamma^+, 2$	543.45(6)	60.8(15)	0.170(95)	$230^{+350}_{-100}$	$E1$	—	$2^{+1}_{-3}$		10
		$3_\gamma^+, 2$	634.56(6)	99.5(25)			$E1$	—	$2.1^{+0.9}_{-3.2}$		
		$2_\gamma^+, 2$	702.84(6)	100(2)			$E1$	—	$1.5^{+0.7}_{-2.3}$		
		$4_{gs}^+, 0$	1442.93(8)	8.6(6)			$E1$	—	$0.01^{+0.01}_{-0.02}$		9
1782.67(10)	$4_2^-, 2$	$5_\gamma^+, 2$	521.53(8)	23.6(16)							
		$3_\gamma^+, 2$	725.19(6)	100(2)							
1805.13(9)	$2_5^+$	$4_1^+, 4$	734.50(6)	44.3(14)	0.055(96)	$> 300$	$E2$	—		$< 76$	6
		$2_\gamma^+, 2$	816.46(6)	100(2)			$E2/M1$	$-0.76^{+0.10}_{-0.13}$		$< 37$	
								$[-3.90^{+0.97}_{-1.34}]$		$< 94$	
1931.96(7)	$2_6^+$	$3_\gamma^+, 2$	874.51(6)	43.4(21)	0.057(39)	$760^{+1800}_{-330}$	$E2/M1$	—		$8^{+3.5}_{-19}$	2, 6
		$4_{gs}^+, 0$	1683.45(7)	45.4(20)			$E2$	—		$0.32^{+0.14}_{-0.75}$	2
		$2_{gs}^+, 0$	1856.65(6)	100(3)			$E2/M1$	$0.92^{+0.41}_{-0.64}$		$0.20^{+0.17}_{-0.47}$	
								$0.50^{+0.87}_{-0.24}$		$0.08^{+0.08}_{-0.31}$	
		$0_{gs}^+, 0$	(1932.00(7))	31.5(17)			$E2$	—		$0.11^{+0.05}_{-0.26}$	
1966.66(10)	$1_3^-$	$2_{gs}^+, 0$	1891.33(6)	100(8)	0.606(48)	$37^{+8}_{-7}$	$E1$	—	$0.84^{+0.28}_{-0.21}$		
						$\tau_{lit} = 19(7)$					
		$0_{gs}^+, 0$	1966.97(13)	57.0(70)			$E1$	—	$0.43^{+0.16}_{-0.11}$		6
2030.90(9)	$(2^+)$	$4_{gs}^+, 0$	1782.14(6)	16.1(22)							
		$2_{gs}^+, 0$	1955.93(7)	100(3)							
2060.43(11)		$0_{gs}^+, 0$	2060.42(6)	100	0.187(44)	$230^{+90}_{-50}$					
2109.32(7)	$1^+$	$3_\gamma^+, 2$	1051.87(6)	47.4(18)	0.138(34)	$330^{+120}_{-70}$	$E2$			$6.2(1.7)$	9, 6
		$2_\gamma^+, 2$	1119.71(13)	57.9(29)			$E2/M1$			$5.6(1.5)$	9
		$2_{gs}^+, 0$	2034.26(6)	100(2)			$E2/M1$			$0.50(13)$	
		$0_{gs}^+, 0$	2109.31(6)	73.3(21)			$M1$				
2135.76(13)		$0_{gs}^+, 0$	2135.74(7)	100	0.111(73)	$420^{+880}_{-180}$					6

*continued*



TABLE I: *continued*

$E_L$ (keV)	$I_i^\pi, K$	$I_f^\pi, K$	$E_\gamma$ (keV)	$L_\gamma$	$F(\tau)$	$\tau$ (fs)	Mult.	$\delta$	$B(E1)$ ( $\times 10^{-3}$ W.u.)	$B(E2)$ (W.u.)	Notes
----------------	--------------	--------------	---------------------	------------	-----------	----------------	-------	----------	-------------------------------------	-------------------	-------

- <sup>1</sup> This  $\gamma$  ray overlaps with an experimental background line, 739.42(5) keV from the  $^{72}\text{Ge}(n, \gamma)$  reaction.
- <sup>2</sup> This  $\gamma$  ray was not used in the level lifetime determination.
- <sup>3</sup> The branching ratios were taken from Ref. [31] and  $\pi_{it}$  was used for the transition probability calculations.
- <sup>4</sup> The  $a_2$  and  $a_4$  values of this  $\gamma$  ray were within uncertainties of Ref. [31] and, therefore, the published  $\delta$  value was used in this work.
- <sup>5</sup> Level lifetime from Ref. [39]; see text for discussion.
- <sup>6</sup> This level or spin assignment adopted from Ref. [31].
- <sup>7</sup> Lifetime reported in Ref. [26].
- <sup>8</sup> Lifetime modified from Ref. [26].
- <sup>9</sup> This  $\gamma$  ray is not reliable for excitation function and/or lifetime determination due to its low intensity.
- <sup>10</sup> This level or spin assignment adopted from Ref. [35].

- [1] A. Aprahamian, Phys. Atom. Nucl. **67**, 1750 (2004).
- [2] X. Wu, A. Aprahamian, S. M. Fischer, W. Reviol, G. Liu, and J. X. Saladin, Phys. Rev. C **49**, 1837 (1994).
- [3] A. Aprahamian, S. R. Leshner, C. Casarella, H. G. Börner, and M. Jentschel, Phys. Rev. C **95**, 024329 (2017).
- [4] P. E. Garrett, M. Kadi, C. A. McGrath, V. Sorokin, M. Li, M. Yeh, and S. W. Yates, Phys. Lett. B **400**, 250 (1997).
- [5] D. Bés, Nucl. Phys. **49**, 544 (1963).
- [6] W.-T. Chou, R. Casten, and P. von Brentano, Phys. Rev. C **45**, 9 (1992).
- [7] R. F. Casten and P. von Brentano, Phys. Rev. C **50**, R1280 (1994).
- [8] P. E. Garrett, J. Phys. G: Nucl. Part. Phys. **27**, R1 (2001).
- [9] J. Smallcombe, P. J. Davies, C. J. Barton, D. G. Jenkins, L. L. Andersson, P. A. Butler, D. M. Cox, R. D. Herzberg, A. Mistry, E. Parr, et al., Phys. Lett. B **732**, 161 (2014).
- [10] P. D. Cottle, M. A. Kennedy, and K. A. Stuckey, Phys. Rev. C **42**, 2005 (1990).
- [11] T. Kibédi and R. H. Spear, Atom. Data Nucl. Data **80**, 35 (2002).
- [12] R. A. Gatenby, J. R. Vanhoy, E. M. Baum, E. L. Johnson, S. W. Yates, T. Belgia, B. Fazekas, A. Veres, and G. Molnár, Phys. Rev. C **41**, R414 (1990).
- [13] L. Bargioni, P. G. Bizzeti, A. M. Bizzeti-Dona, D. Bazzacco, S. Lunardi, P. Pavan, C. Rossi-Alvarez, G. de Angelis, G. Maron, and J. Rico, Phys. Rev. C **51**, R1057 (1995).
- [14] L. Caballero, B. Rubio, P. Kleinheinz, S. W. Yates, A. Algorta, A. Dewald, A. Fitzler, A. Gadea, J. Jolie, R. Julin, et al., Phys. Rev. C **81**, 031301(R) (2010).
- [15] P. Kleinheinz, J. Styczen, M. Piiparinen, J. Blomqvist, and M. Kortelahti, Phys. Rev. Lett. **48**, 1457 (1982).
- [16] S. Lunardi, P. Kleinheinz, M. Piiparinen, M. Ogawa, M. Lach, and J. Blomqvist, Phys. Rev. Lett. **53**, 1531 (1984).
- [17] M. Piiparinen, P. Kleinheinz, J. Blomqvist, A. Virtanen, A. Atac, D. Muller, J. Nyberg, T. Ramsøy, and G. Sletten, Phys. Rev. Lett. **70**, 150 (1993).
- [18] C. Küppersbusch, S. Pascu, P. von Brentano, D. Buscurescu, Gh. Căta-Danil, D. Deleanu, J. Endres, M. Elvers, D. Filipescu, C. Friebner, et al., Eur. Phys. J. A **48**, 1 (2012).
- [19] F. Corminboeuf, J. Jolie, H. Lehmann, K. Föhl, F. Hoyler, H. G. Börner, C. Doll, and P. E. Garrett, Phys. Rev. C **56**, R1201 (1997).
- [20] C. Fahlander, A. Axelsson, M. Heinebrodt, T. Härtlein, and D. Schwalm, Phys. Lett. B **388**, 475 (1996).
- [21] H. G. Börner, J. Jolie, F. Hoyler, S. J. Robinson, B. Krusche, R. Piepenbring, R. F. Casten, A. Aprahamian, and J. P. Draayer, Phys. Rev. Lett. **66**, 691 (1991).
- [22] M. Oshima, T. Morikawa, Y. Hatsukawa, S. Ichikawa, N. Shinohara, M. Matsuo, H. Kusakari, N. Kobayashi, M. Sugawara, and T. Inamura, Phys. Rev. C **52**, 3492 (1995).
- [23] T. Härtlein, M. Heinebrodt, D. Schwalm, and C. Fahlander, Eur. Phys. J. A **2**, 253 (1998).
- [24] P. E. Garrett, M. Kadi, Min. Li, C. A. McGrath, V. Sorokin, M. Yeh, and S. W. Yates, Phys. Rev. Lett. **78**, 4545 (1997).
- [25] A. Aprahamian, R. C. de Haan, S. R. Leshner, J. Döring, A. M. Bruce, H. G. Börner, M. Jentschel, and H. Lehmann, J. Phys. **G25**, 685 (1999).
- [26] S. R. Leshner, C. Casarella, A. Aprahamian, B. P. Crider, R. Ikeyama, I. R. Marsh, M. T. McEllistrem, E. E. Peters, F. M. Prados-Estévez, M. K. Smith, et al., Phys. Rev. C **91**, 054317 (2015).
- [27] P. E. Garrett, N. Warr, and S. W. Yates, J. Res. Natl. Inst. Stand. Technol. **105**, 141 (2000).
- [28] P. E. Garrett, H. Lehmann, J. Jolie, C. A. McGrath, M. Yeh, W. Younes, and S. W. Yates, Phys. Rev. C **64**, 024316 (2001).
- [29] E. E. Peters, A. Chakraborty, B. P. Crider, B. H. Davis, M. K. Gnanamani, M. T. McEllistrem, F. M. Prados-Estévez, J. R. Vanhoy, and S. W. Yates, Phys. Rev. C **88**, 024317 (2013).
- [30] E. Shelton and V. C. Rodgers, Comput. Phys. Commun. **6**, 99 (1973).
- [31] L. I. Govor, A. M. Demidov, V. A. Kurkin, and I. V. Mikhailov, Yad. Fiz. **72**, 1799 (2009).
- [32] T. Belgia, G. Molnár, and S. W. Yates, Nucl. Phys. A **607**, 43 (1996).

- [33] K. B. Winterbon, Nucl. Phys. **A246**, 293 (1975).
- [34] C. W. Reich, Nucl. Data Sheets **105**, 557 (2005).
- [35] E. P. Grigoriev, Phys. Atom. Nucl. **75**, 1427 (2012).
- [36] Y. Yoshizawa, B. Elbek, B. Herskind, and M. C. Olesen, Nucl. Phys. **73**, 273 (1965).
- [37] C. Baktash, J. X. Saladin, J. O'Brien, I. Y. Lee, and J. E. Holder, Phys. Rev. C **10**, 2265 (1974).
- [38] R. Ronningen, J. Hamilton, A.V.Ramayya, L. Varnell, G. Garcia-Bermudez, J. Lange, W. Lourens, L. Riedinger, R. Robinson, P. Stelson, et al., Phys. Rev. C **15**, 1671 (1977).
- [39] F. K. McGowan and W. T. Milner, Phys. Rev. C **23**, 1926 (1981).
- [40] T. Ichihara, H. Sakaguchi, M. Nakamura, M. Yosoi, M. Ieiri, Y. Takeuchi, H. Togawa, T. Tsutsumi, and S. Kobayashi, Phys. Rev. C **36**, 1754 (1987).
- [41] Y. Y. Berzin, E. P. Grigorév, and T. V. Guseva, Bull. Acad. Sci. USSR, Phys. Ser. **53**, 76 (1989).
- [42] S. Pascu, D. Buscurescu, G. Căta-Danil, V. Derya, M. Elvers, D. Filipescu, D. G. Ghită, T. Glodariu, A. Hennig, C. Mihai, et al., Phys. Rev. C **91**, 034321 (2015).
- [43] A. Aprahamian, Phys. Rev. C **46**, 2093 (1992).
- [44] L. M. Robledo and G. F. Bertsch, Phys. Rev. C **84**, 054302 (2011).
- [45] L. M. Robledo and G. F. Bertsch, Phys. Rev. C **86**, 054306 (2012).
- [46] K. Nomura, R. Rodríguez-Guzmán, and L. M. Robledo, Phys. Rev. C **92**, 014312 (2015).
- [47] W. Korten, P. Brocking, H. Hubel, W. Pohler, U. van Severen, P. Willsau, T. Haertlein, C. Ender, P. Reiter, D. Schwalm, et al., Z. Phys. **A351**, 143 (1995).
- [48] K. Neergård and P. Vogel, Nucl. Phys. A **145** (1970).
- [49] A. F. Barfield, J. L. Wood, and B. R. Barrett, Phys. Rev. C **34**, 2001 (1986).
- [50] R. H. Spear, Atom. Data Nucl. Data **42**, 55 (1989).
- [51] D. P. DiPrete, E. L. Johnson, E. M. Baum, C. A. McGrath, D. Wang, M. F. Villani, S. W. Yates, T. Belgia, B. Fazekas, and G. Molnár, Phys. Rev. C **52**, R2831 (1995).

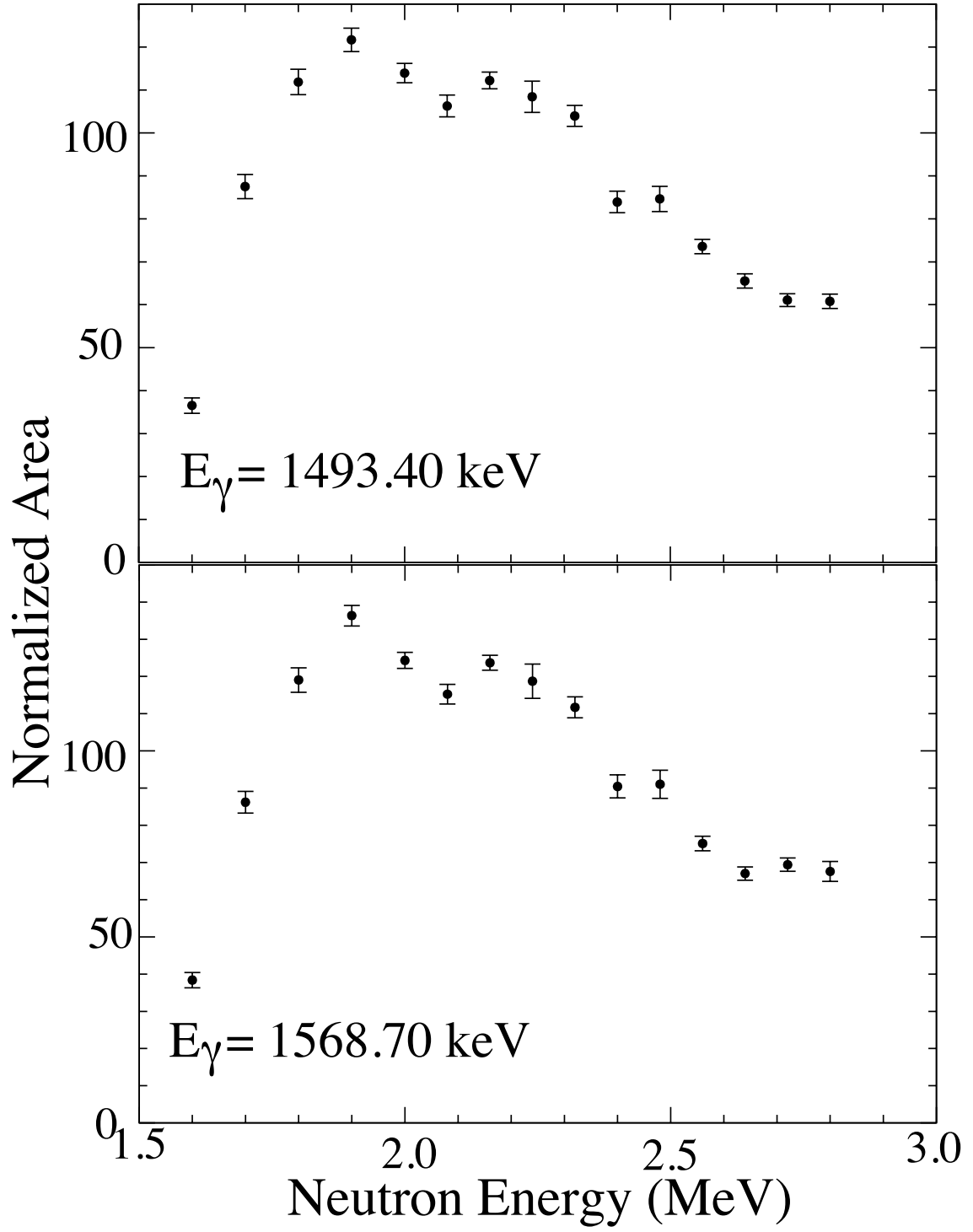


FIG. 1: Excitation functions for the 1493.40- and 1568.70-keV  $\gamma$  rays originating from the 1568.77-keV level. Both exhibit the same excitation energy threshold and overall shape.

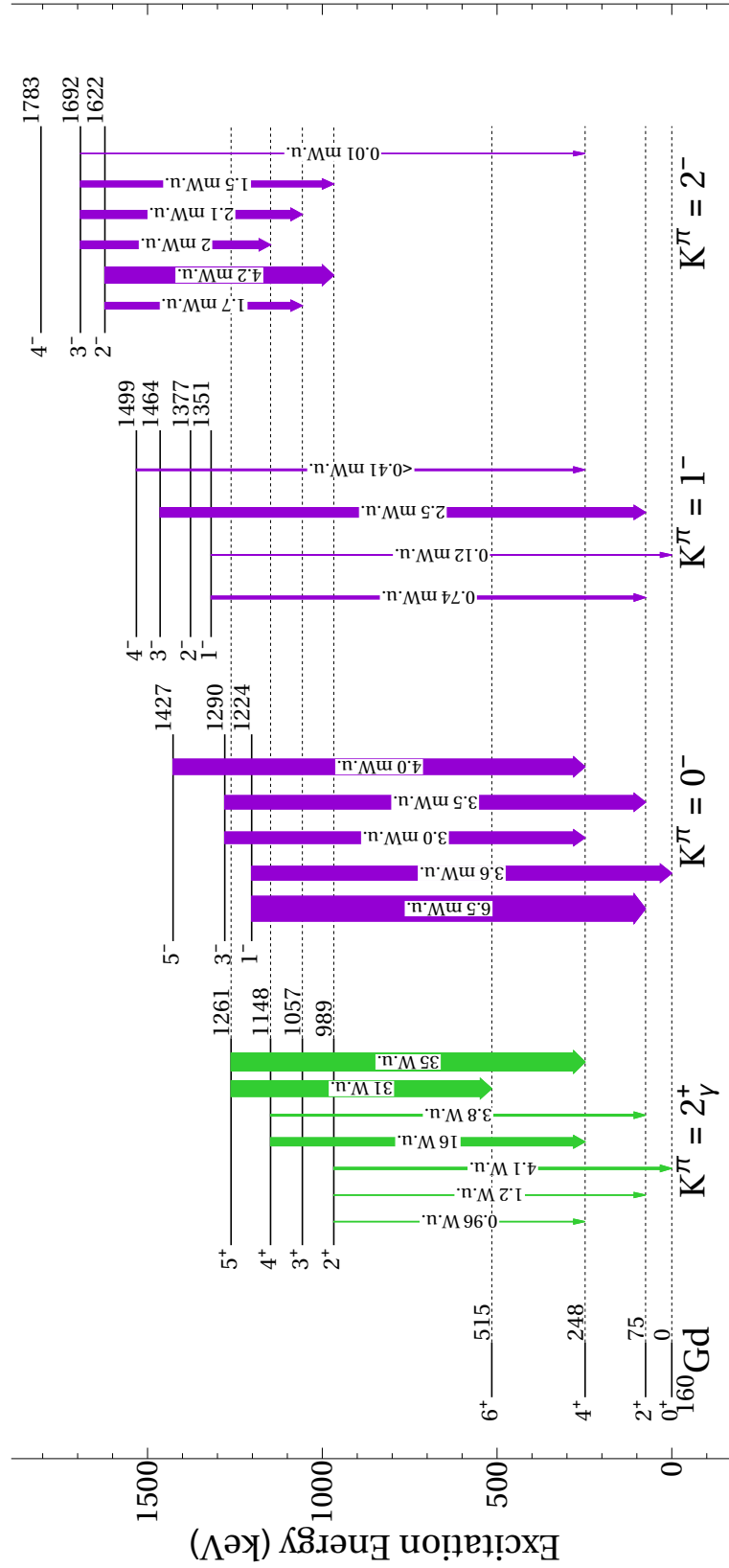


FIG. 2: (color online) A partial level scheme of  $^{160}\text{Gd}$  highlighting the  $K^\pi = 2^+$   $\gamma$  and negative-parity bands. The  $B(E2)$  values in W.u. are shown in green and  $B(E1)$  values in mW.u. in purple and scaled separately. All values are also listed in Table I.

FIG. 3: (color online) A level scheme of  $^{160}\text{Gd}$  highlighting the  $K^\pi = 0^+$  bands. The  $B(E2)$  values in W.u. are shown in green and  $B(E1)$  values in mW.u. in purple and are scaled separately. All values are also listed in Table I.

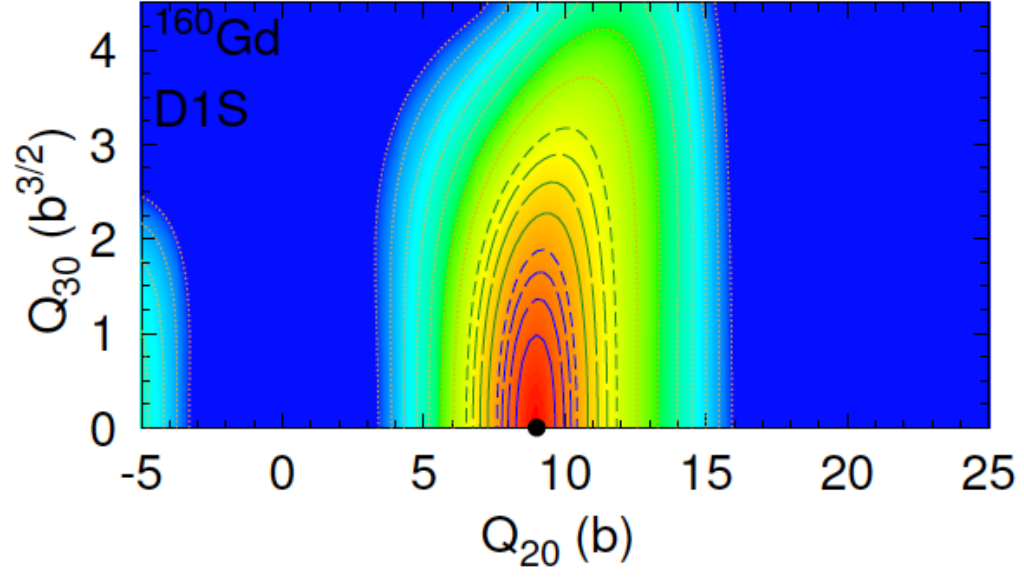


FIG. 4: (color online) Potential energy surface as a function of the quadrupole and octupole degrees of freedom for  $^{160}\text{Gd}$ . The dot is located at the ground-state minimum.

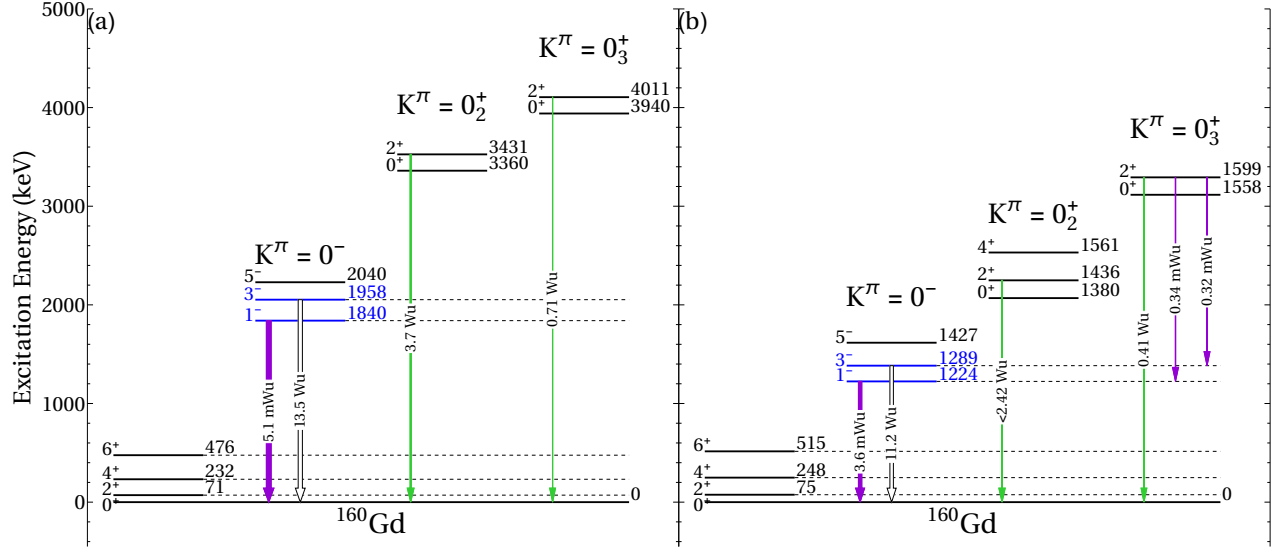


FIG. 5: (color online) Partial level schemes for  $^{160}\text{Gd}$ . The  $B(E2)$  values in W.u. are shown in green,  $B(E1)$  values in mW.u. in purple, and  $B(E3)$  values in W.u. in white outlined in black. The two level schemes are scaled separately. a) GCM calculations using the Gogny D1S energy density functional is shown along with calculated transition probabilities. In this calculation, the first excited  $K^\pi = 0^-$  state appears at an excitation energy of 1.84 MeV and a  $B(E1; 1_{K^\pi=0^-}^- \rightarrow 0_{gs}^+)$  value of 5.1 mW.u. The  $B(E3; 3^- \rightarrow 0_{gs}^+) = 13.50$  W.u. The second excited state is a one-phonon  $\beta$  vibration with an excitation energy of 3.36 MeV and the  $2^+$  member decays to the ground state with a  $B(E2; 2^+ \rightarrow 0_{gs}^+) = 3.7$  W.u. The third excited  $K^\pi = 0^+$  band is a two-octupole phonon at 3.94 MeV, and  $B(E2; 2^+ \rightarrow 0_{gs}^+) = 0.71$  W.u. The GCM calculation predicts a double-octupole excited  $K^\pi = 0^+$  band at 3.9 MeV built on the  $K^\pi = 0^-$  band at 1840 keV. b) The experimental partial level scheme with experimental transition probabilities. The  $B(E3; 3^- \rightarrow 0_{gs}^+)$  for the 1289-keV level is taken from Ref. [39].